

Supplementary Information

Core-shell (nano-SnX/nano-Li₄Ti₅O₁₂)@C spheres (X=Se,Te) with high volumetric capacity and excellent cycle stability for lithium-ion batteries

Xuebu Hu,^{*a} Biao Shang,^a Tianbiao Zeng,^a Qimeng Peng,^a Gang Li,^a Yongjin Zou,^b and Yuxin Zhang^c

^aCollege of Chemistry and Chemical Engineering, Chongqing University of Technology, Chongqing 400054, China

^bGuangxi Key Laboratory of Information Materials, Guilin University of Electronic Technology, Guilin 541004, China

^cState Key Laboratory of Mechanical Transmissions, College of Materials Science and Engineering, Chongqing University, Chongqing 400044, China

^{*}Corresponding author

Email: xuebu@cqut.edu.cn; Tel: +86-23-62563250; Fax: +86-23-62563221

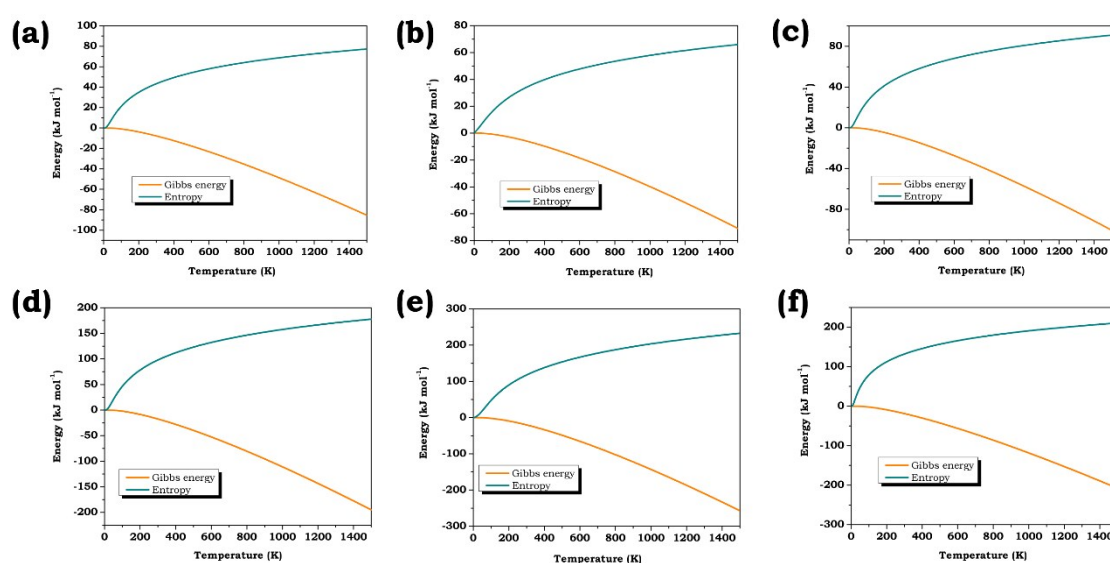


Fig. S1 Calculated Enthalpy and Gibbs free energy of (a) Sn, (b) Se, (c) Te, (d) SnSe, (e) SnSe₂

and (f) SnTe.

Fig. S2a displays the calculated thermodynamics result. This diagram shows the Gibbs free energy of the reactions as a function of temperature, assuming the kinetics are favorable, a reaction proceeds as we expect if $\Delta G < 0$. The result indicate that Se, Te and Sn can be in chemical combination to generate SnSe and SnTe at room temperature condition because the Δ Gibbs free energy $< 0 \text{ kJ mol}^{-1}$. But in fact SnSe and SnTe will not generate when Sn, Se and Te powder are just mixed, thus, outer energy is needed to support the reaction occurrence. The results of ΔG indicate that SnSe and SnSe₂ will form at different temperature. Therefore, temperature needs to be controlled accurately. For the investigation of proper selenization and tellurization temperature, (Sn/LTO)@C is annealed with Se or Te powder at different temperatures (350, 450, and 550 °C), as shown in Fig. S2b, SnSe and SnTe can be obtained when the reaction temperature is set at 350 °C, however, small amount of SnSe₂ is also generated. When the reaction temperature increased from 350 °C to 450°, the peaks intensity of SnSe and SnTe are increasing slowly. With the temperature increase to 550 °C, SnSe₂ convert to SnSe completely. Compared with 350 and 450 °C, the temperature of 550 °C actually provides more energy to the system, which promotes the complete conversion of Sn and Se into SnSe. For the synthesis process of SnTe, Sn and Te will also be gradually converted into SnTe when the temperature goes up to 550 °C. The XRD results demonstrate that pure SnSe and SnTe can be synthesize at the opted temperature of 550 °C.

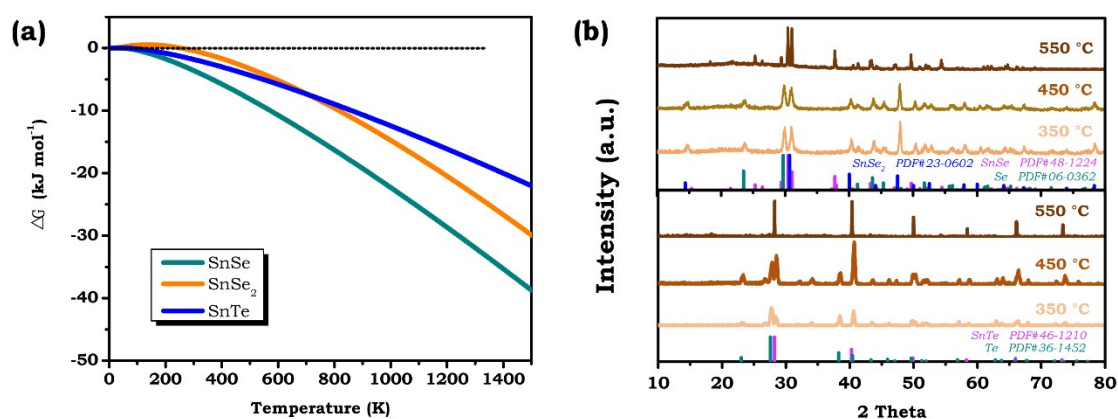


Fig. S2 (a) The calculated Δ Gibbs free energy of the reactions (b) XRD results of Sn/Se/C and Sn/Te/C at different temperatures

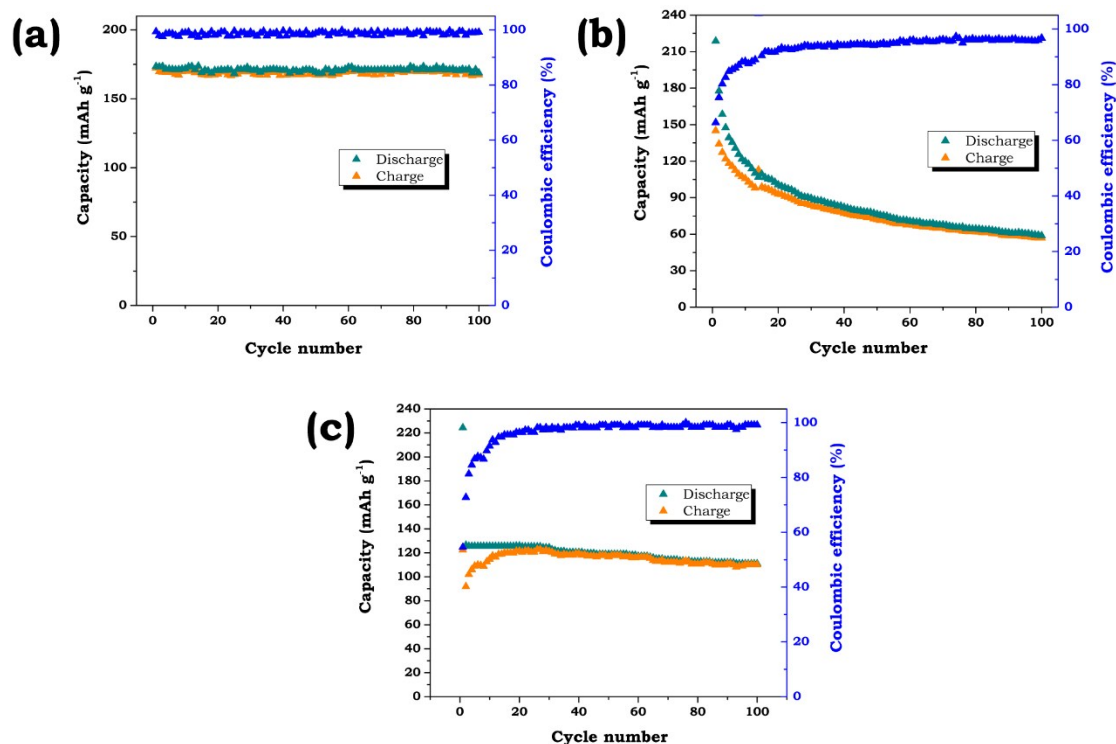


Fig. S3 Cycles performance of (a) LTO, (b) pyrolytic carbon and (c) acetylene black at 200 mA g⁻¹

1

Nitrogen adsorption-desorption isotherms of the (n-SnSe/n-LTO)@C (Fig. S4a) and the (n-SnTe/n-LTO)@C (Fig. S4c) show type-IV characteristics, which is typical of mesoporous structures.¹ These isotherms are obtained with a large Brunauer-Emmett-Teller (BET) surface area of 64.1 m² g⁻¹ and 70.3 m² g⁻¹ for (n-SnSe/n-LTO)@C and (n-SnTe/n-LTO)@C respectively. Moreover, two dominant peak at 2.7 nm for (n-SnSe/n-LTO)@C and 2.4 nm of (n-SnTe/n-LTO)@C are observed in the pore size distribution, which reveals the existence of the mesoporous in the composite. The high specific surface area and mesoporous of the composite would help to accommodate the volume fluctuations during the discharge/charge processes and improve the electrolyte penetration and ion diffusion, thus resulting in enhanced electrochemical performance in LIBs.²

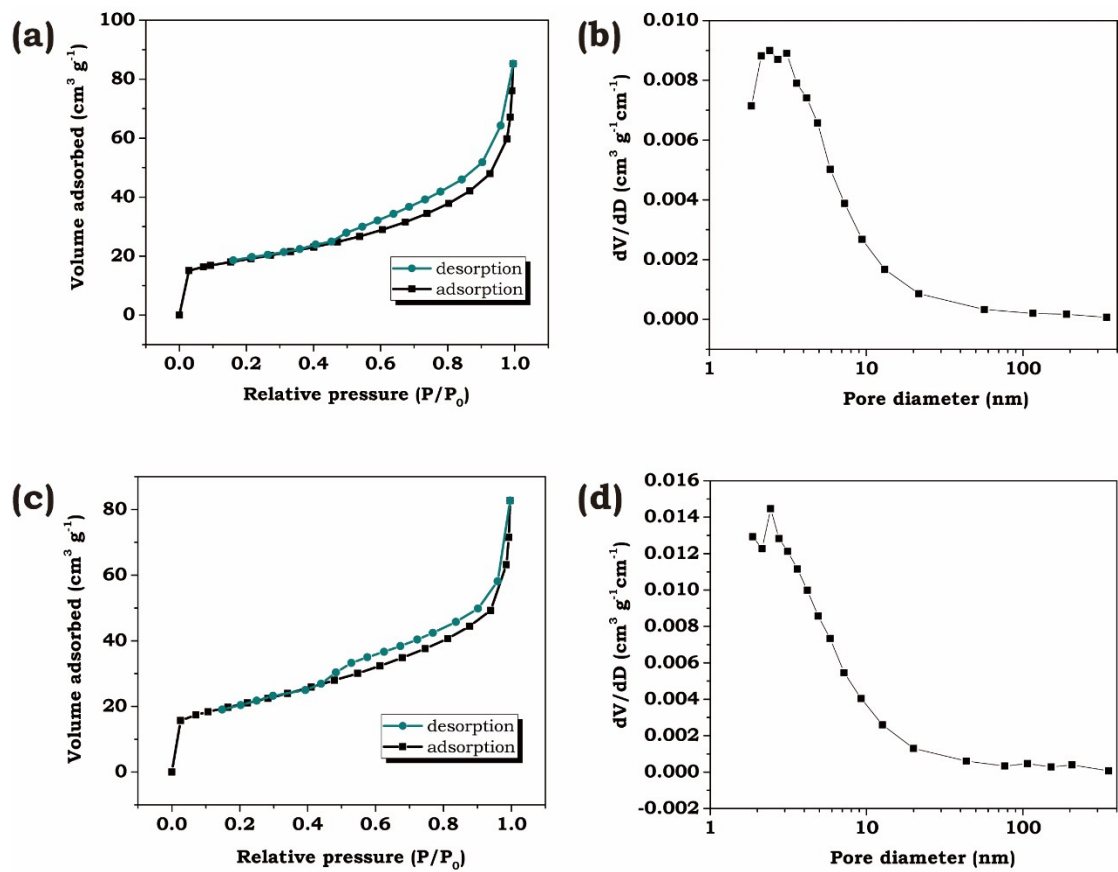


Fig. S4 Nitrogen adsorption-desorption isotherms and pore size distributions of (a, b) (n-SnSe/n-LTO)@C and (c, d) (n-SnTe/n-LTO)@C.

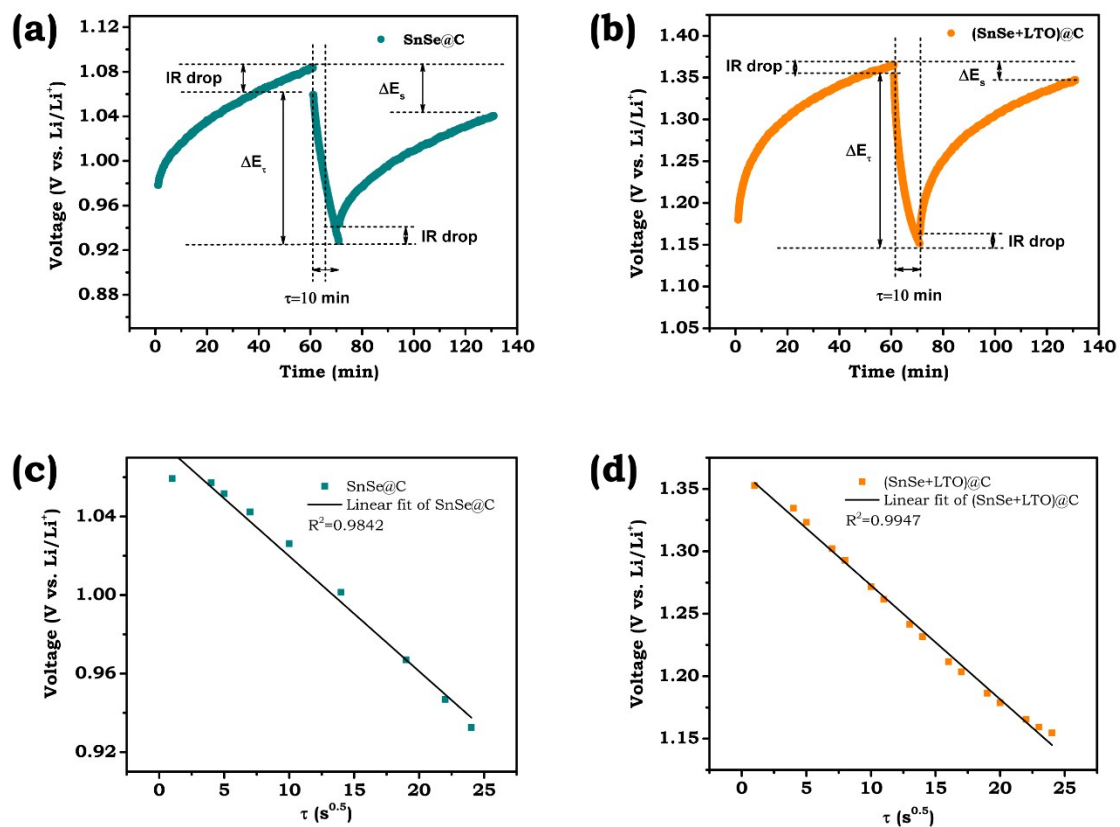


Fig. S5 A magnified single step during GITT measurement marked with τ , ΔE_s , and ΔE_{τ} parameters of (a) SnSe@C and (b) (n-SnSe/n-LTO)@C. Linearly fitted voltage response with respect to square root of time for (c) SnSe@C and (d) (n-SnSe/n-LTO)@C.

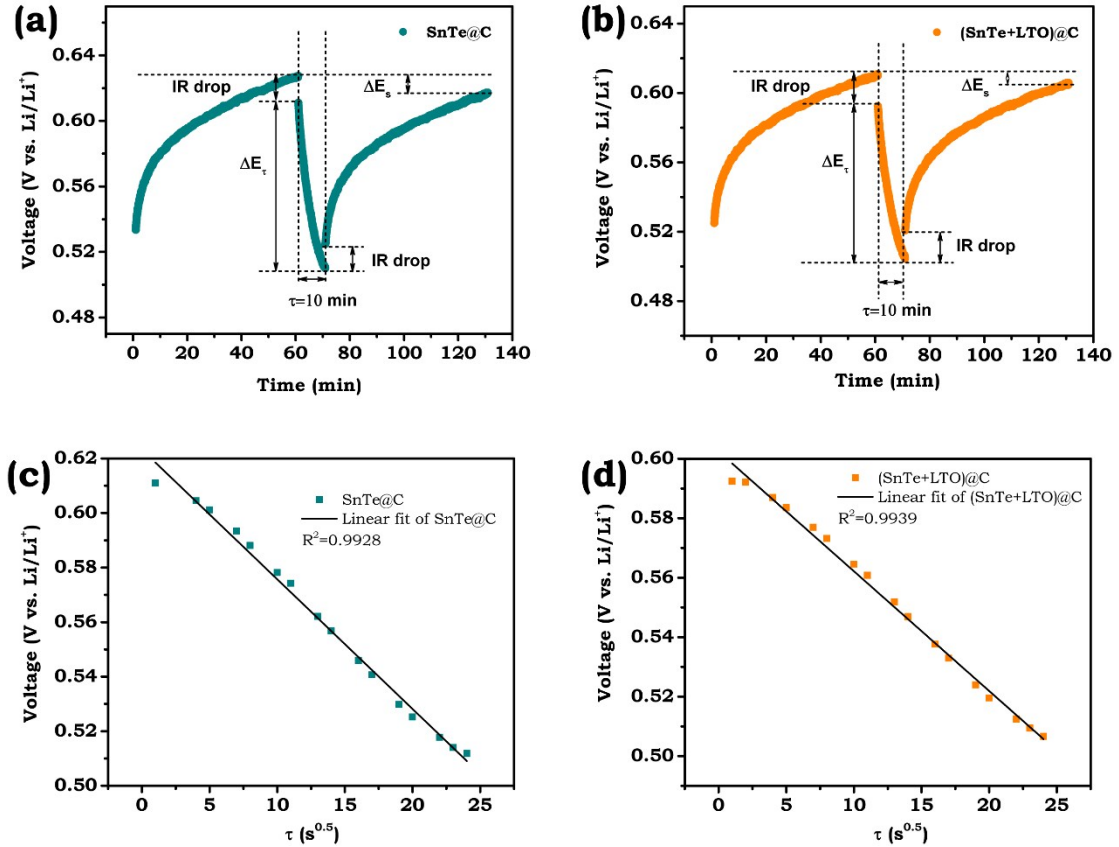


Fig. S6 A magnified single step during GITT measurement marked with τ , ΔE_s , and ΔE_t parameters of (a) SnTe@C and (b) (n-SnTe/n-LTO)@C. Linearly fitted voltage response with respect to square root of time for (c) SnTe@C and (d) (n-SnTe/n-LTO)@C.

The ac impedance and cyclic voltammetry have been done and the results are shown in Fig. S7 and S8. As shown in the Fig. S7, in (n-SnSe/LTO)@C, cathodic peaks at low voltage (< 1.3 V) are associated with lithium alloying with Sn forming a Li_xSn alloys.³ Anodic peaks around 0.5 V are assigned to the dealloying reaction of Li_xSn alloys. The peaks at 1.7~2.0 V may be due to the formation of SnSe.^{4, 5} In (n-SnTe/LTO)@C, cathodic peaks centered at ~ 1.1 V during the discharge process, which are associated with the alloying reaction between Te and Li^+ to form the Li_2Te phase. Upon the charge process, the anodic peak centered at ~ 1.6 V is detected, corresponding to the dealloying reaction of Li_2Te phase, and the recombination of SnTe phase.⁶ In addition, three anodic peaks at approximately 0.3 ~ 0.5 V are detected as well, illustrating the dealloying of the Li_xSn phase.⁷

As shown in the Fig. S8, the value of R_{ct} in all electrodes is bigger after 10 cycles compared with the first cycle in all electrodes. In addition, (n-SnSe/LTO)@C and (n-SnTe/LTO)@C

electrodes show smaller increase of R_{ct} after the tenth cycle than those of bare SnSe and SnTe, indicating the good stability of the interface between the active materials and electrolyte, which proves the advantages of the electrode structure.

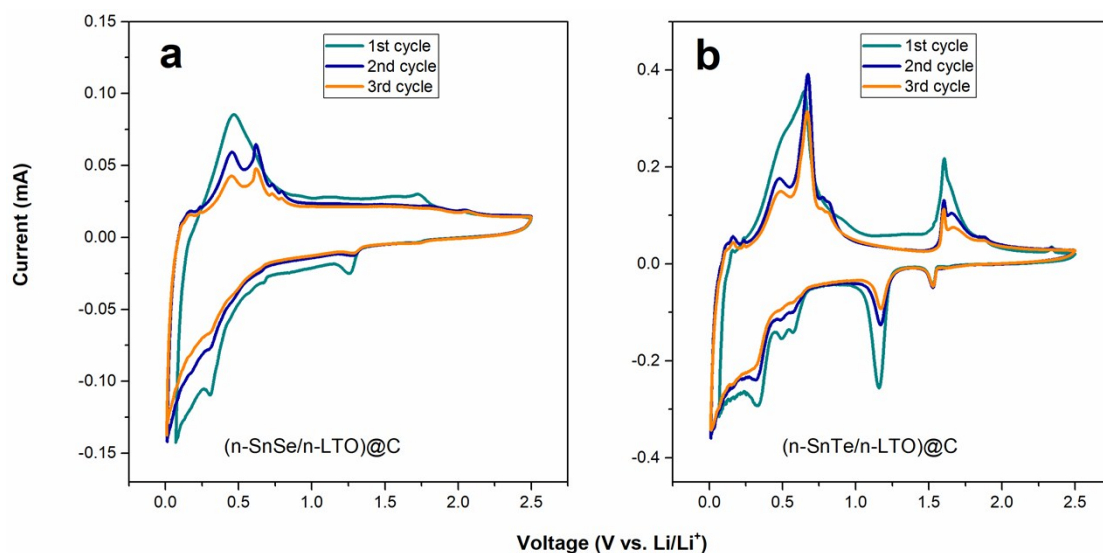


Fig. S7 CV curves of (a) (n-SnSe/n-LTO)@C and (b) (n-SnTe/n-LTO)@C at 0.1 mV s^{-1} .

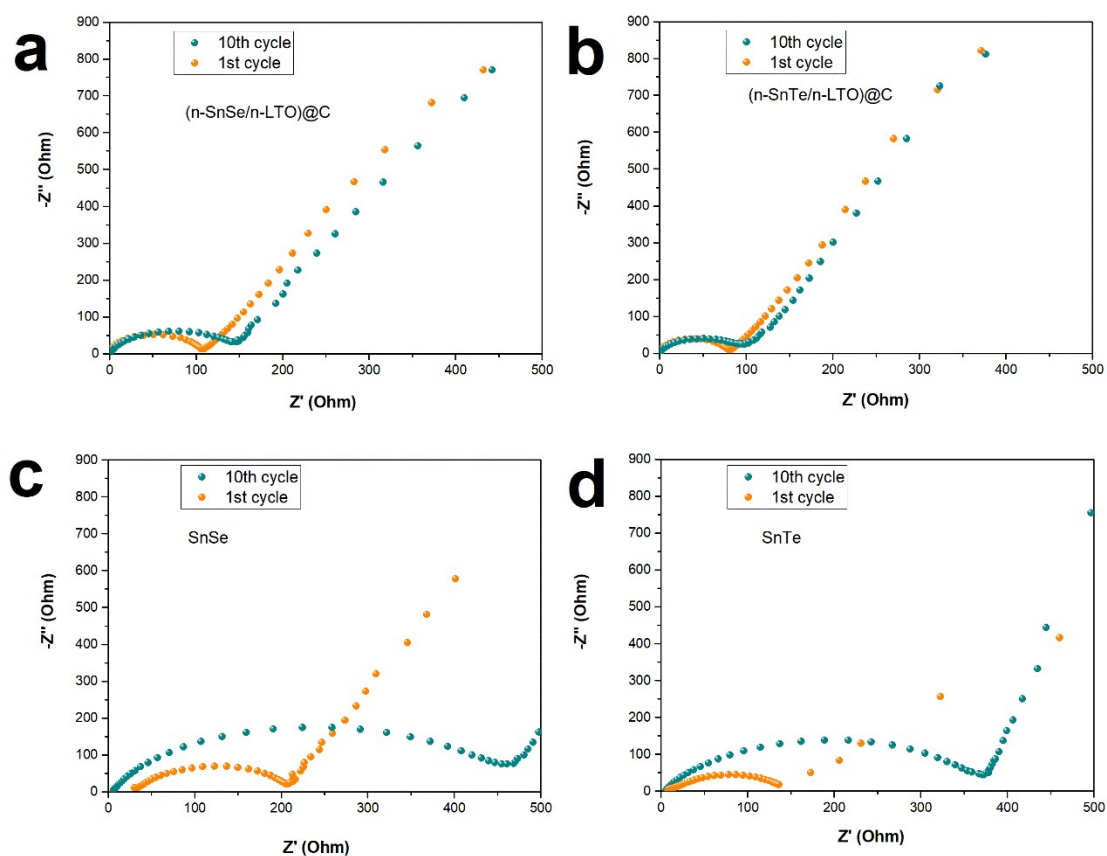


Fig. S8 Electrochemical impedance spectra (EIS) of the cells with (a) (n-SnSe/n-LTO)@C, (b) (n-

SnTe/n-LTO)@C, (c) bare SnSe and (d) bare SnTe electrodes after the 1st and 10th cycles.

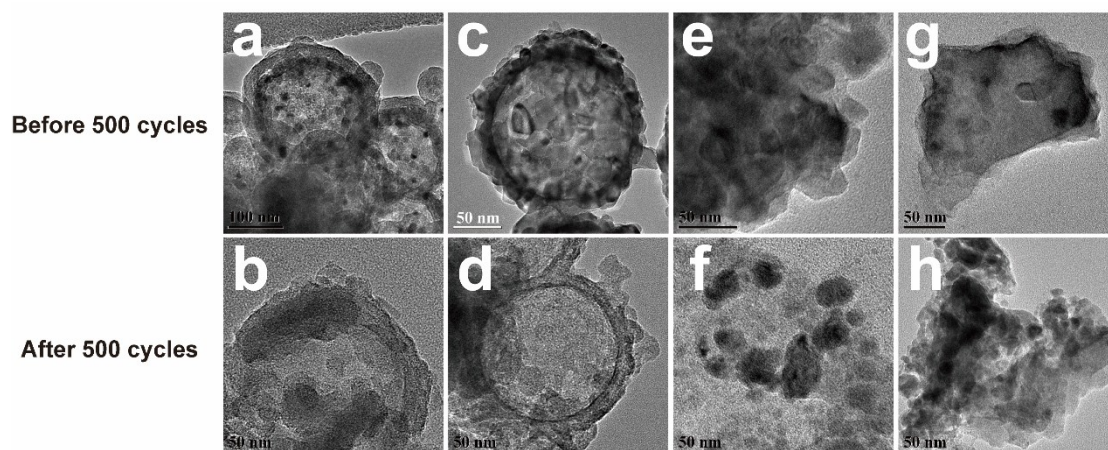


Fig. S9 TEM images of (n-SnSe/n-LTO)@C (a,b), (n-SnTe/n-LTO)@C (c,d), SnSe (e,f) and SnTe (g,h) before and after 500 cycles at 1.0 A g⁻¹.

Table S1 The mass content of each component in the samples tested by ICP measurement

Sample	Component	ICP(wt.%)	
		X=Se	X=Te
(n-SnX/n-LTO)@C	Sn	55.30	45.20
	Ti	2.70	2.00
	Li	0.31	0.22
	SnX*	92.10	93.80
	LTO*	5.30	3.80
	C*	2.60	2.40

* These values were calculated by ICP

References:

1. H. Xu, L. Qin, J. Chen, Z. Wang, W. Zhang, P. Zhang, W. Tian, Y. Zhang, X. Guo and Z. Sun, *J. Mater. Chem. A*, 2018, **6**, 13153-13163.
2. Y. Chen, X. Yuan, C. Yang, Y. Lian, A. A. Razzaq, R. Shah, J. Guo, X. Zhao, Y. Peng and Z. Deng, *J. Alloys Compd.*, 2019, **777**, 127-134.
3. Zhang, L. Lu, D. C. Zhang, W. T. Hu, N. Wang, B. Xu, Y. M. Li and H. Zeng, *Electrochimica Acta*, 2016, **209**, 423-429.

4. Z. Xue, J. Yao, S. C. Cheng and Z. W. Fu, *Journal of the Electrochemical Society*, 2006, **153**, A270-A274.
5. Zhang, X. Zhao and J. Li, *Electrochimica Acta*, 2015, **176**, 1296-1301.
6. A. Grishanov, A. A. Mikhaylov, A. G. Medvedev, J. Gun, P. V. Prihodchenko, Z. J. Xu, A. Nagasubramanian, M. Srinivasan and O. Lev, *Energy Technology*, 2018, **6**, 127-133.
7. Y. Son, J. Hur, K. H. Kim, H. B. Son, S. G. Lee and I. T. Kim, *Journal of Power Sources*, 2017, **365**, 372-379.